

Morphodynamics of barchan and dome dunes under variable wind regimes

Xin Gao¹, Cyril Gadal², Olivier Rozier², and Clément Narteau²

¹State Key Laboratory of Desert and Oasis Ecology, Xinjiang Institute of Ecology and Geography, Chinese Academy of Sciences, 818 South Beijing Road, Urumqi 830011, Xinjiang, China

²Institut de Physique du Globe de Paris, Sorbonne Paris Cité, Université Paris Diderot, UMR 7154 CNRS, 1 rue Jussieu, 75238 Paris Cedex 05, France

ABSTRACT

Dome dunes are traditionally interpreted as a transient or an independent class of bedforms because of their rounded and smooth shape without slipfaces. Here we show that they can also reach a steady state and form dome dune fields, which entail the same interactions between flow, bed topography, and moving sediment as other dune types in the absence of grain-size segregation and vegetation. We study the transition from barchan to dome dunes by increasing the standard deviation of a normal distribution of sand flux orientation in a numerical model. We find that, under steady-state conditions, barchan and dome dunes exhibit the same relationships between their height and migration rate. As shown in Earth's deserts, dome dune shape and migration rate can then be used to estimate sand flux properties, including the variability in transport directionality.

INTRODUCTION

Frequently observed in dune systems on Earth and Mars, dome dunes are isolated sand piles with a rounded or oblong smooth shape and no slipface (Holm, 1953; Hastings, 1994; de Hon, 2006; Bourke et al., 2008). Although usually incipient or disappearing dunes, they can also form vast dune fields and reach a giant size with superimposed bedforms (Fig. 1A). Nevertheless, unlike other dune types, dome dunes cannot be classified according to the orientation

and/or the sinuosity of their crest lines. Hence, they have not been the subject of much research and there are still uncertainties about the conditions under which they develop.

The dome dune morphology has been associated with the presence of coarse grains (McKee, 1966, p. 26), vegetation (Goldsmith, 1985) or cohesion (Schatz et al., 2006), but none of these environmental factors have been recognized as a critical ingredient. Furthermore, dome dunes frequently coexist with either barchan or linear

dunes along sediment transport pathways (Figs. 1B–1D). Mainly observed in zones of low sediment availability, a population of dome dunes generally exhibits a regular pattern with a characteristic length scale. The shape and the size of dome dunes are not random and, as with other dune types, their formation and movement are likely to reflect the local wind conditions. For example, dome dunes have been reported under bidirectional wind regimes, in laboratory and modeling experiments, with divergence angles $< 90^\circ$ and periods of flow reorientation much shorter than the dune turnover time (Parteli et al., 2009; Reffet et al., 2010).

The relation between dune shape and wind regime has always been a major issue in aeolian geomorphology (Wasson and Hyde, 1983). In the vast majority of cases, dunes show a specific orientation, which can be theoretically related to two independent dune-growth mechanisms according to sand availability (Courrech du Pont et al., 2014; Gao et al., 2015; Lucas et al., 2015). For both mechanisms, whether dunes grow in

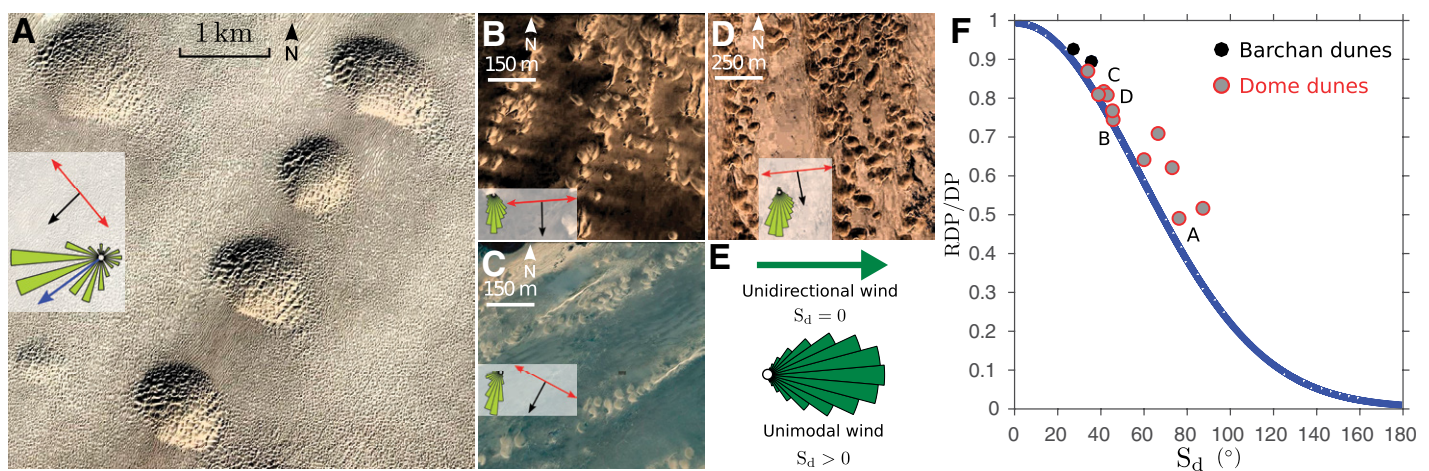


Figure 1. Dome dunes and the variability in sand flux orientation in terrestrial dune systems. **A:** Giant dome dunes in the northern Taklamakan Desert (China, $40^\circ 14'N$, $83^\circ 31'E$). The sand flux rose is derived from the wind data of Xiaotang meteorological station ($40^\circ 49'N$, $84^\circ 17'E$). Blue arrow shows the resultant drift direction. **B,C:** Barchan, linear, and dome dunes in Mauritania ($20^\circ 28'N$, $16^\circ 17'W$; $21^\circ 07'N$, $14^\circ 07'W$). **D:** A dome dune field in Egypt ($24^\circ 30'N$, $27^\circ 07'E$). Insets show sand flux roses and dune orientations associated with the two dune growth mechanisms. Images from GoogleEarth™. **E:** Sand flux roses for unidirectional and unimodal wind regimes using a normal distribution of sand flux orientation with a resultant transport from west to east and a standard deviation, S_d . **F:** The RDP/DP (resultant drift potential [RDP] and drift potential [DP]) with respect to the variability S_d of sand flux orientation in different terrestrial dune fields (points) and for a normal distribution of sand flux orientation (line).

height from a sedimentary bed or elongate on a non-erodible ground from a localized sand source, fluctuations in flow and transport properties permanently alter the shape of individual dunes (Tsoar, 1984; Elbelrhiti et al., 2005; Elbelrhiti and Douady, 2011). It appears that in addition to the succession of seasonal winds with distinct orientations (Zhang et al., 2012; Lü et al., 2017), the dispersion of sand flow around a given orientation could be an important control parameter for the selection of dune shape and orientation. Such a dispersion has been largely ignored in dune physics, and its impact on dune morphodynamics remains to be investigated. Given their smooth shapes, dome dunes can be regarded as the ideal dune type to start these investigations.

Here we analyze the relationship between wind regimes and steady-state dome dune properties in different terrestrial dune systems using satellite imagery and the surface winds predicted by global atmospheric reanalysis data. We compare these observations to the output of a numerical dune model, in which the sole free parameter is the standard deviation of a normal distribution of sand flux orientation. Thus, we study the transition from barchan to dome dunes, and show how transport properties can be derived from field observations (i.e., dune shape and migration rate).

METHODS

We studied 12 barchan and dome dune fields on Earth (in northern Africa and China; Fig. DR1 in the GSA Data Repository¹). For each dune field, the distribution of sand flux orientation was derived from the 10 m surface wind data provided by the ERA-Interim project (Dee et al., 2011) and the transport law proposed by Ungar and Haff (1987). These distributions were used to compute the resultant drift direction, the standard deviation of sand flux orientation, the ratio RDP/DP between the resultant drift potential (RDP; i.e., the norm of the mean sand flux vector) and the drift potential (DP; i.e., the mean of the norms of the individual sand flux vectors), as well as the two dune orientations associated with the two dune growth mechanisms (see the Data Repository). These parameters were also derived from local wind data for the giant dome dune field in the northern Taklamakan Desert, China (Fig. 1A).

¹GSA Data Repository item 2018272, DRI (wind data, transport properties and dune orientations in terrestrial dune systems); DRII (estimation of dune asymmetry); DRIII (model of dune contour); DRIV (formation of steady-state dune patterns in the numerical dune model); DRV (growth rate with respect to dune orientation under unimodal wind regimes); and DRVI (steady-state dome dune morphodynamics in Mauritania, is available online at <http://www.geosociety.org/datarepository/2018/> or on request from editing@geosociety.org.

From satellite imagery, we extracted the contour shape of at least 20 dunes at each site to estimate the dune shape asymmetry; i.e., the coefficient of variation of the distances between the center of mass (centroid) of a dune and points regularly spaced on its contour (Fig. DR2). This quantity is able to capture the transition from crescentic to rounded shapes and, for comparison, we introduced a simple geometric parameterization for dune contour. According to the resultant drift direction, the upstream part of the contour in this geometric model is always the semicircle of diameter $AB = 2r$. The downstream part of the contour is an arc of chord AB with a sagitta a that varies from $-r$ to r . Then, the dune contour is a semicircle for $a = 0$. It takes a crescentic and an ovoid shape for $-r < a < 0$ and $0 < a < r$, respectively (Fig. DR3).

We ran numerical simulations using a cellular automaton dune model (Narteau et al., 2009; Rozier and Narteau, 2014). In all simulations, the resultant drift direction remained the same, but we changed the standard deviation, S_d , of a normal distribution of sand flux orientation (Fig. 1E). In practice, we considered 200 successive winds with the same speed but different orientations. Expressed in the time scale t_0 of the model, individual winds blow for $t_0 = 20 t_0$, and the period of wind reorientation is $T = 4 \times 10^3 t_0$. The initial condition is a circular source of sediment with a diameter of $15 l_0$ or a conical sand pile with a radius of $60 l_0$ and a height of $40 l_0$, where l_0 is the elementary length scale of the cellular space. For simulations with a localized sand source, we employed open boundary conditions, and the input flux varied according to local transport rates as we maintained a layer of sedimentary cells above the circular source that is embedded in the flat non-erodible ground. To reach a steady state starting from conical sand piles, all the sediment ejected downstream was randomly reinjected upstream. In addition, the volume of conical sand piles was three orders of magnitude larger than the volume of sediment transported over t_0 to ensure that the dune kept a “memory” of its shape over the period of wind reorientation. When a statistical steady state was reached, we estimated the dune migration rate as well as the dune asymmetry using the same method as in terrestrial dune fields.

MORPHODYNAMICS OF DOME DUNES

Figure 1F shows the RDP/DP with respect to the standard deviation of sand flux orientation for the different dune fields under investigation, and a normal distribution of sand flux orientation. The close agreement between the data and the theoretical relationship indicates that, in the selected dune fields, a normal distribution can simulate most of the variability in transport directionality. There is a transition from barchan to dome dunes when S_d approaches 40° . This

S_d corresponds to a RDP/DP of 0.8, a threshold value commonly proposed to limit the domains of occurrence of barchan and linear dunes in bidirectional wind regimes (Tsoar, 1984). Here we find that the same threshold value can be used to differentiate the domains of occurrence of barchan and dome dunes under unimodal wind regimes.

The steady-state dune patterns predicted by the simulations are presented in Figures 2A and 2B. For narrow unimodal wind regimes, $S_d < 30^\circ$, crescentic barchan dunes with permanent slipfaces orientated perpendicularly to the resultant transport direction were systematically observed. From $S_d = 30^\circ$ to $S_d = 50^\circ$, there is a transition from barchan to dome dunes, and the slipface tends to disappear over the period of wind reorientation. For $S_d > 30^\circ$, dome dunes with circular or elliptical shapes are the only steady-state dune patterns, but transient linear dune features may align with the resultant drift direction (Fig. DR4). In simulations starting from a conical sand pile (Fig. 2A), the average sand flux between

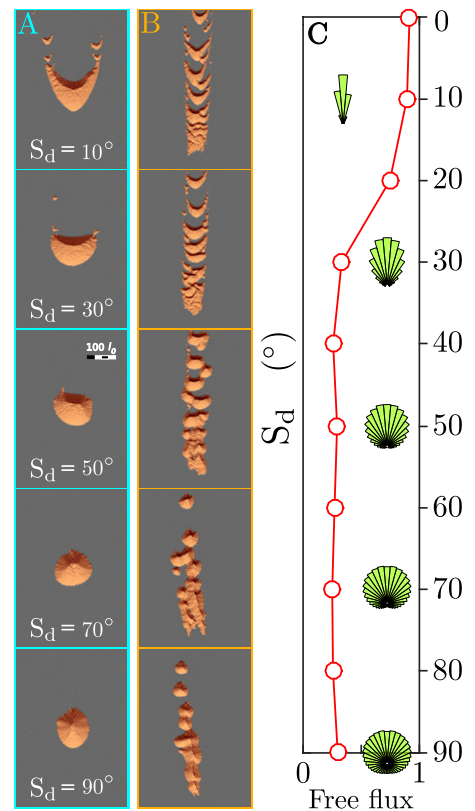


Figure 2. Dune patterns with respect to the variability of sand flux orientation (standard deviation, S_d) in the numerical model. A: Steady-state barchan and dome dunes starting from a conical sand pile. B: Trains of barchan and dome dunes migrating on a non-erodible ground from a localized sand source. C: The average sand flux between dome dunes in the numerical simulation, the so-called free flux, normalized by its value at $S_d = 0^\circ$. Sand flux roses show the normal distribution of sand flux orientation.

dunes, the so-called free flux, captures the transition from barchan to dome dunes (Fig. 2C). Surprisingly, the rounded shape of dome dunes under wide unimodal wind regimes are associated with a smaller free flux than the crescentic shape of barchan dunes under narrow unimodal wind regimes.

Figure 3A shows how the dune shape of terrestrial and modeled dunes depends on the S_d of sand flux orientation. The more complex shapes measured in the field come from the diversity of factors that affect dune shape in Earth's deserts compared to the over-simplistic nature of the model (e.g., collisions, topography; Bourke, 2010). Nevertheless, both dune types exhibit similar variations, which can be illustrated and quantified by measuring the contour shape using our simple geometric parameterization (black line in Fig. 3A).

Re-scaled with respect to the resultant transport (i.e., the RDP), the migration rate of barchan and dome dunes in the model has the same dependence on height (Fig. 3B). This agrees with the classical law for barchan dune migration (Zhang et al., 2010), confirming that the increase in wind velocity at the top of steady-state dunes in the model, the so-called fractional speed-up ratio, is close to 1.6 (see inset in Fig. 3B), a reasonable value for terrestrial dune systems.

DISCUSSION

Dome dunes have always been considered as an independent class of bedforms because of their smooth and rounded shapes. However, contrary to bedforms associated with grain-size segregation (i.e., zibars [coarse-grained, low-relief eolian bedforms with a large spacing but without slipfaces]) or vegetation (i.e., parabolic and blowout dunes), the emergence of dome dunes requires the same interactions between flow and granular material as all other elementary dune types (i.e., barchan, linear, or star dunes). Therefore, their specificity relies only on the absence of distinct crest line orientation. We show here that this can be the result of a wide variation in sand flux orientation. Under such conditions, the difference in growth rate between the different dune orientations is too small to select a particular alignment (Fig. DR5). Nevertheless, the orientations associated with the two dune growth mechanisms can be recognized in both modeled and terrestrial dome dune fields using transient features such as slipfaces or linear ridges.

Another mechanism responsible for the rounded and smooth shape of dome dunes is related to sediment loss just after a wind reorientation. Indeed, horns or flat terminations shaped by previous winds are likely to rapidly erode under a new wind orientation, temporarily increasing the output flux from the dunes. This behavior is presented in Figure 4 for steady-state dome dune fields in Mauritania and in a model, where transient linear ridges escape from the

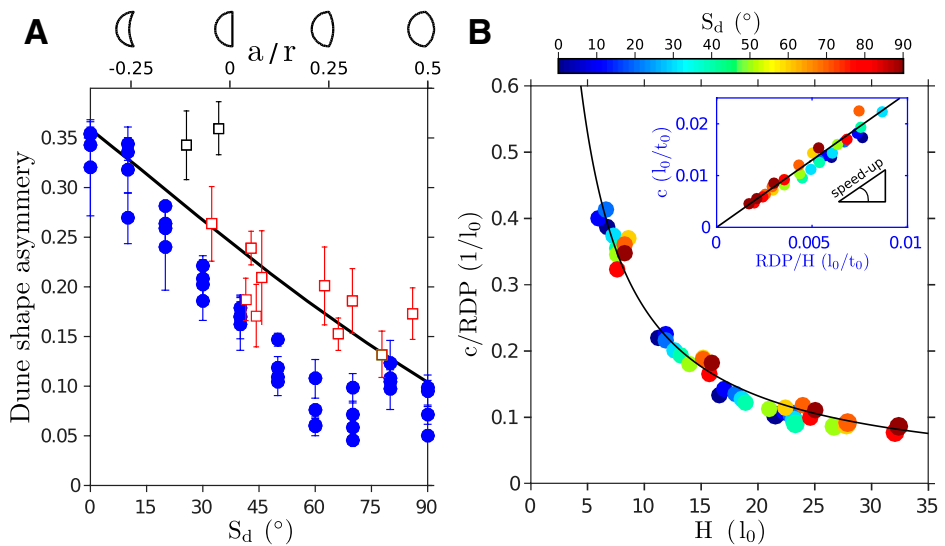


Figure 3. Morphodynamics of dome dunes. A: Asymmetry of the contour shape with respect to the standard deviation (S_d) of sand flux orientation. Black and red squares represent terrestrial barchan and dome dune fields, respectively: error bars show the variability computed for at least 20 dunes for each studied site. Blue dots represent modeled dunes: error bars show the variability over time of the steady-state dune shape. Black curve corresponds to the geometric model of the contour shape shown in the top axis. B: Migration rate of steady-state dunes with respect to their height in the numerical simulations starting from a conical sand pile (Figure 2A). Inset shows the migration rate with respect to the ratio between the resultant transport and the height. Adjusting the fractional speed-up ratio γ , black lines are the best fits to the data using the classical law for dune migration speed $c = Q_{\text{crest}}/H = (1 + \gamma)RDP/H$, where Q_{crest} is the resultant sand flux at the crest and l_0 is the elementary length scale of the cellular space. The slope $1 + \gamma = 2.6$ is shown in the inset.

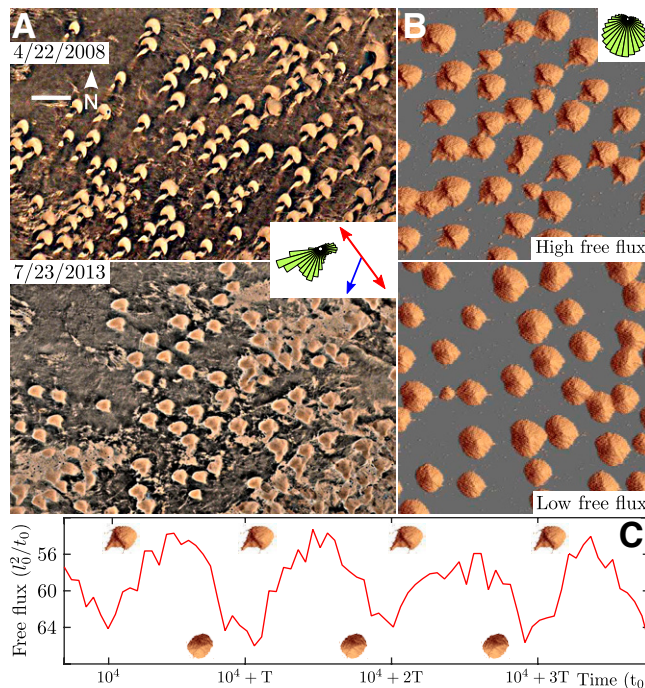


Figure 4. Evolution of dome dune fields. A: Dome dune field in Mauritania ($18^{\circ}59'N$, $14^{\circ}09'W$; image from GoogleEarth™) at two different times. Insets show sand flux roses and dune orientations associated with the two dune growth mechanisms. B: Steady-state dome dune field at two different times in the numerical model for standard deviation $S_d = 60^{\circ}$. The initial condition is a flat sand bed with a thickness of $2l_0$. C: Evolution of the free flux in the simulation shown in B. Transient elongated structures are ejected from the dune over a short time after a wind reorientation, periodically increasing the free flux.

dunes following a change in wind orientation. Therefore, the circular shape of dome dunes can be considered as the morphology for which the overall sediment loss is minimized. Considering steady-state bedforms, it naturally explains why the free flux in dome dune fields under wide unimodal wind regimes is smaller than in barchan

dune fields (Figs. 4B and 4C). As shown by Bristow and Lancaster (2004), this is not the case for isolated, disappearing dome dunes ejected at the tip of giant linear dunes.

This study suggests that it is necessary to account for the variation in sand flux orientation in order to document the variety of dune

shapes. For example, the transition from barchan to dome dunes illustrated here under variable wind regimes could be representative of similar transitions for linear and star dunes under bimodal and multimodal wind regimes, respectively (Zhang et al., 2012; Gao et al., 2015). In addition, it is likely that the variability of wind directionality will also generate various types of secondary features, mainly associated with the coexistence of the two dune growth mechanisms and changes in defect density or crest-line sinuosity.

The numerical model predicts that steady-state barchan and dome dunes have the same dynamic properties governed by the principle of mass conservation. However, in the absence of a slipface, and for an increasing standard deviation of sand flux orientation, the transverse components of transport on the rounder shape of dome dunes have an increasing contribution to the overall transport rate. Therefore, direct measurements of the contour shape, size, and migration rate of dome dunes in nature can be used to estimate transport properties, including the variability of sand flux orientation. From the two satellite images shown in Figure 4A (in Mauritania, 18°59'N, 14°09'W), we measured the migration rate and the length of 210 dome dunes. For a windward slope angle of 10°, the slope of the relationship between the migration rate and the inverse of dune height gives a resultant transport at the crest of 42.9 m²/yr (Fig. DR6). This value agrees with the field observations of Ahmedou et al. (2007), resultant sand flux at the crest, $Q_{\text{crest}} \approx 50$ m²/yr, and with the resultant transport direction derived from the surface wind data of the ERA-Interim project (RDP = 20.4 m²/yr) using the classical range of fractional speed-up ratio between 0.8 ($Q_{\text{crest}} = 36.2$ m²/yr) and 2 ($Q_{\text{crest}} = 61.2$ m²/yr). Using the dune asymmetry measured in the field, the theoretical relationships shown in Figures 3A and 1F give a standard deviation of 62° ± 8° for the distribution of sand flux orientation, and a RDP/DP value between 0.47 and 0.64. This again agrees with the RDP/DP of 0.51 computed from the wind provided by the climate model.

CONCLUSIONS

In this study, we have started to document the impact of the variation in sand flux orientation on dune patterns. Considering only a normal distribution of sand flux orientation, we characterize the transition between barchan and dome dunes. The comparison between field observations and numerical experiments shows how dome dune morphodynamics (i.e., size, shape, migration rate) are sensitive to variability in sand flux orientation. We conclude that, in combination with other dune types (barchan, linear, and star dunes),

dome dunes could serve as a working template to integrate the variability of wind directionality in eolian geomorphology. However, a number of important issues remain for future investigation. The most important are related to the seasonal variability in wind orientation, and the impact of the variability of sand flux in several prevailing wind orientations.

ACKNOWLEDGMENTS

The data presented in this paper are the result of numerical simulations using ReSCAL, the Real-Space Cellular Automaton Laboratory (<http://rescal.geophysx.org>). The source codes can be downloaded from <http://www.ipgp.fr/rescal>. We acknowledge financial support from the National Thousand Talents Program of China (grant Y772091001), the High-level Talent Recruitment Program of Xinjiang Uygur Autonomous Region (grant Y742071001), “the Belt and Road” Special Project (grant 131965KYB20170038), the UnivEarthS LabEx program of Sorbonne Paris Cité (grants ANR-10-LABX-0023 and ANR-11-IDEX-0005-02), and the French National Research Agency (grant ANR-17-CE01-0014/SONO).

REFERENCES CITED

Ahmedou, D.O., Mahfoudh, A.O., Dupont, P., El Moutar, A.O., Valance, A., and Rasmussen, K.R., 2007, Barchan dune mobility in Mauritania related to dune and interdune sand fluxes: *Journal of Geophysical Research*, v. 112, F02016, <https://doi.org/10.1029/2006JF000500>.

Bourke, M.C., Edgett, K.S., and Cantor, B., 2008, Recent aeolian dune change on Mars: *Geomorphology*, v. 94, p. 247–255, <https://doi.org/10.1016/j.geomorph.2007.05.012>.

Bourke, M.C., 2010, Barchan dune asymmetry: Observations from Mars and Earth: *Icarus*, v. 205, p. 183–197, <https://doi.org/10.1016/j.icarus.2009.08.023>.

Bristow, C., and Lancaster, N., 2004, Movement of a small slipfaceless dome dune in the Namib Sand Sea, Namibia: *Geomorphology*, v. 59, p. 189–196, <https://doi.org/10.1016/j.geomorph.2003.09.015>.

Courrech du Pont, S., Narteau, C., and Gao, X., 2014, Two modes for dune orientation: *Geology*, v. 42, p. 743–746, <https://doi.org/10.1130/G35657.1>.

de Hon, R., 2006, Transitional dune forms on Mars: 37th Lunar and Planetary Science Conference, 13–17 March 2006, League City, Texas, Abstract 1361, <https://www.lpi.usra.edu/meetings/lpsc2006/pdf/1361.pdf>.

Dee, D., et al., 2011, The ERA-interim reanalysis: Configuration and performance of the data assimilation system: *Quarterly Journal of the Royal Meteorological Society*, v. 137, p. 553–597, <https://doi.org/10.1002/qj.828>.

Elbelrhiti, H., Claudin, P., and Andreotti, B., 2005, Field evidence for surface-wave-induced instability of sand dunes: *Nature*, v. 437, p. 720–723, <https://doi.org/10.1038/nature04058>.

Elbelrhiti, H., and Douady, S., 2011, Equilibrium versus disequilibrium of barchan dunes: *Geomorphology*, v. 125, p. 558–568, <https://doi.org/10.1016/j.geomorph.2010.10.025>.

Gao, X., Narteau, C., Rozier, O., and Courrech du Pont, S., 2015, Phase diagrams of dune shape and orientation depending on sand availability: *Scientific Reports*, v. 5, p. 14677, <https://doi.org/10.1038/srep14677>.

Goldsmith, V., 1985, Coastal dunes, in Davis Jr., R.A., ed., *Coastal Sedimentary Environments*: New

York, Springer-Verlag, p. 303–378, https://doi.org/10.1007/978-1-4612-5078-4_5.

Hastings, K., 1994, The dynamics of barchans and dome dunes Namib Desert, Namibia [Ph.D. thesis]: Wollongong, Australia, University of Wollongong, 147 p.

Holm, D.A., 1953, Dome-shaped dunes of central Nejd, Saudi Arabia: *Proceedings of the 19th International Geological Congress*, Algiers, p. 107–112.

Lü, P., Narteau, C., Dong, Z., Rozier, O., and Courrech du Pont, S., 2017, Unravelling raked linear dunes to explain the coexistence of bedforms in complex dunefields: *Nature Communications*, v. 8, p. 14239, <https://doi.org/10.1038/ncomms14239>.

Lucas, A., Narteau, C., Rodriguez, S., Rozier, O., Calot, Y., Garcia, A., and Courrech du Pont, S., 2015, Sediment flux from the morphodynamics of elongating linear dunes: *Geology*, v. 43, p. 1027–1030, <https://doi.org/10.1130/G37101.1>.

McKee, E.D., 1966, Structures of dunes at White Sands National Monument, New Mexico: *Sedimentology*, v. 7, p. 3–69, <https://doi.org/10.1111/j.1365-3091.1966.tb01579.x>.

Narteau, C., Zhang, D., Rozier, O., and Claudin, P., 2009, Setting the length and time scales of a cellular automaton dune model from the analysis of superimposed bed forms: *Journal of Geophysical Research*, v. 114, F03006, <https://doi.org/10.1029/2008JF001127>.

Parteli, E.J., Durán, O., Tsoar, H., Schwämmle, V., and Herrmann, H.J., 2009, Dune formation under bimodal winds: *Proceedings of the National Academy of Sciences of the United States of America*, v. 106, p. 22085–22089, <https://doi.org/10.1073/pnas.0808646106>.

Reffet, E., Courrech du Pont, S., Hersen, P., and Douady, S., 2010, Formation and stability of transverse and longitudinal sand dunes: *Geology*, v. 38, p. 491–494, <https://doi.org/10.1130/G30894.1>.

Rozier, O., and Narteau, C., 2014, A real-space cellular automaton laboratory: *Earth Surface Processes and Landforms*, v. 39, p. 98–109, <https://doi.org/10.1002/esp.3479>.

Schatz, V., Tsoar, H., Edgett, K.S., Parteli, E.J.R., and Herrmann, H.J., 2006, Evidence for indurated sand dunes in the martian north polar region: *Journal of Geophysical Research: Planets*, v. 111, E04006, <https://doi.org/10.1029/2005JE002514>.

Tsoar, H., 1984, The formation of seif dunes from barchans—A discussion: *Zeitschrift für Geomorphologie*, v. 28, p. 99–103.

Ungar, J., and Haff, P., 1987, Steady state saltation in air: *Sedimentology*, v. 34, p. 289–299, <https://doi.org/10.1111/j.1365-3091.1987.tb00778.x>.

Wasson, R., and Hyde, R., 1983, Factors determining desert dune types: *Nature*, v. 304, p. 337–339, <https://doi.org/10.1038/304337a0>.

Zhang, D., Narteau, C., Rozier, O., and Courrech du Pont, S., 2012, Morphology and dynamics of star dunes from numerical modelling: *Nature Geoscience*, v. 5, p. 463–467, <https://doi.org/10.1038/ngeo1503>.

Zhang, D., Narteau, C., and Rozier, O., 2010, Morphodynamics of barchan and transverse dunes using a cellular automaton model: *Journal of Geophysical Research*, v. 115, F03041, <https://doi.org/10.1029/2009JF001620>.

Manuscript received 1 May 2018
 Revised manuscript received 6 July 2018
 Manuscript accepted 7 July 2018

Printed in USA